University of Michigan School of Public Health

The University of Michigan Department of Biostatistics Working Paper Series

Year 2006 *Paper* 56

Detecting Pulsatile Hormone Secretion Events: A Bayesian Approach

Tim Johnson*

*University of Michigan Biostatistics, tdjtdj@umich.edu

Detecting Pulsatile Hormone Secretion Events: A Bayesian Approach

Tim Johnson

Abstract

Many challenges arise in the analysis of pulsatile, or episodic, hormone concentration time series data. Among these challenges is the determination of the number and location of pulsatile events and the discrimination of events from noise. Analyses of these data are typically performed in two stages. In the first stage, the number and approximate location of the pulses are determined. In the second stage, a model (typically a deconvolution model) is fit to the data conditional on the number of pulses. Any error made in the first stage is carried over to the second stage. Furthermore, current methods, except two, assume that the underlying basal concentration is constant. We present a fully Bayesian deconvolution model that simultaneously estimates the number of secretion episodes, as well as their locations, and a non-constant basal concentration. This model obviates the need to determine the number of events a priori. Furthermore, we estimate probabilities for all "candidate" event locations. We demonstrate our method on a real data set.

Detecting Pulsatile Hormone Secretion Events: A Bayesian Approach

Timothy D. Johnson*

Abstract

Many challenges arise in the analysis of pulsatile, or episodic, hormone concentration time series data. Among these challenges is the determination of the number and location of pulsatile events and the discrimination of events from noise. Analyses of these data are typically performed in two stages. In the first stage, the number and approximate location of the pulses are determined. In the second stage, a model (typically a deconvolution model) is fit to the data conditional on the number of pulses. Any error made in the first stage is carried over to the second stage. Furthermore, current methods, except two, assume that the underlying basal concentration is constant. We present a fully Bayesian deconvolution model that simultaneously estimates the number of secretion episodes, as well as their locations, and a non-constant basal concentration. This model obviates the need to determine the number of events, a priori. Furthermore, through processing of the posterior distribution, probabilities can be estimated for all "candidate" event locations. We demonstrate our method on a real data set.

KEY WORDS: Bayesian analysis, BDMCMC, b-spline, deconvolution, ill-posed inverse problem, non-stationary time series, Dirichlet process prior, latent point process, marked point process.

*email: tdjtdj@umich.edu, tel. (734) 936-1007

1 Introduction

Hormones are the main vehicle used in distant cell-to-cell communication throughout the human body. For example, gonadotropic hormones, produced and secreted into the circulatory system by the pituitary gland, signal distant target cells in the gonads. These, in turn, produce sex hormones that are responsible for the changes seen during puberty and for the monthly menstrual cycles in healthy, young, mature women. The timing and amount of hormone secreted into the circulatory system is thus vital to normal functioning of many physiological processes and many diseases are associated with a disruption of the normal patterns of hormone release.

For example, 26 clinically depressed women and 26 matched controls were enrolled in a study at the University of Michigan. Women were admitted to the General Clinical Research Center for a twenty-four hour period of observation, commencing at nine in the morning, during which time blood was drawn at ten minute intervals. The serum was subsequently assayed for cortisol, a stress related hormone. One question of interest was whether the secretion pattern was disrupted in depressed women (Young, Carlson, and Brown, 2001).

The secretion of hormones into the circulatory system can be broadly classified into two categories: oscillatory and pulsatile. An example of oscillatory hormone secretion is the diurnal pattern of Dopamine. Other hormones, including cortisol, a stress related hormone produced by the adrenal glands, are released in a pulsatile fashion (Berne and Levy, 1993), as can be seen from the concentration profile in the upper left panel of Figure 1. Furthermore, there is evidence that cortisol has an underlying oscillatory component, on top of which, the pulsatile release of hormone is superimposed (Veldhuis et al., 1989).

Many methods for pulse identification have been proposed and subsequently classified into criterion-based and model-based methods (Mauger and Brown, 1995). Criterion-based models (see, e.g., Veldhuis and Johnson, 1986; Merriam and Wachter, 1982; Oerter, Guardabasso, and Rodbard, 1986; Van Cauter et al., 1981) are typically used to determine the location of pulses. Model-based methods assume some model for the data (see, e.g., O'Sullivan and

O'Sullivan, 1988; Diggle and Zeger, 1989; Kushler and Brown, 1991; Veldhuis and Johnson, 1992; Komaki, 1993; Guo, Wang, and Brown, 1999; Johnson, 2003; Yang, Liu, and Wang, In Press). In an extensive simulation study Mauger and Brown (1995) showed that model-based methods are preferred over criterion-based methods on the grounds of false positive and false negative error rates.

Many model-based methods use criterion-based methods to identify initial pulses or to select several competing models (three exceptions are Diggle and Zeger (1989) Guo, Wang, and Brown (1999) and Johnson (2003)). Thus, an error in the initial identification of a pulse is carried over to the model-based methods that rely on them. Further, only two previous methods have incorporated a changing basal concentration along with pulse identification/parameter estimation (Guo, Wang, and Brown, 1999; Yang, Liu, and Wang, In Press). All other methods assume a zero basal concentration or, at most, a constant basal concentration. Thus, if information such as the amount of hormone secreted per pulse is of interest, then not accounting for the changing basal secretion will tend to over estimate this quantity. Lastly, a recent study (Keenan and Veldhuis, 2003) suggests that pulse size and shape vary throughout the day. Only two models have allowed for this biologic variation in pulse shape and size (Johnson, 2003; Yang, Liu, and Wang, In Press).

To date, no model has been proposed that 1) does not rely on the initial identification of pulses; 2) accounts for both pulsatile and oscillatory components of hormone release; and 3) models variation in pulse shape and size. In this paper, we present a fully Bayesian approach that addresses these three issues. Our method extends earlier work by Johnson (2003) and O'Sullivan and O'Sullivan (1988).

We present our model in the Section 2. Then we briefly discuss some issues related to posterior simulation in Section 3. We analyze an example cortisol data set from the aforementioned study in Section 4. In Section 5, we discuss posterior estimation of event probabilities and compare results from our model with the nonlinear mixed effects partial spline model (NMPSM) developed by Yang, Liu, and Wang (In Press). We consider several

different error structures in Section 6 and conclude with a discussion in Section 7.

2 The Bayesian Deconvolution Model

We now present the Bayesian deconvolution model (BDM). The biophysical model presented below follows that in Yang, Liu, and Wang (In Press). We begin with the likelihood.

2.1 The likelihood

Let Y_j denote the observed concentration at time t_j. Our estimation procedure does not require that the observed times series be equally spaced in time. Let ε_t denote the error at time t, let $C(t_j)$ denote the true concentration at time t_j. Then Y_j is related to the concentration $C(t_j)$ by

$$\begin{aligned} \ln(Y_j) &= \ln[C(t_j)] + \varepsilon_j \\ \varepsilon_j &\overset{iid}{\sim} N(0, \sigma^2), \quad j = 1, \ldots, n \end{aligned} \tag{1}$$

where n is the number of observations in the time series. We model the log of the concentration for several reasons. First, the true concentration is always non-negative as is the observed concentration from assay. Second, it has been argued (Rodbard, Rayford, and Ross, 1970) that since the error in concentration is a combination of several different sources of error, including assay, biological and dilution errors, a symmetric error structure is inappropriate. (1) implies that the observed concentration has a lognormal distribution, which is non-negative. Third, assay error is commonly a function of the level of the hormone. It is common to assume that the $\varepsilon_t \sim N(0, \sigma^2)$, independently of one another. However, we will allow for more general error structures in Section 6. In particular, let $\boldsymbol{\varepsilon} = (\varepsilon_1, \ldots, \varepsilon_n)^{\mathrm{T}}$; then $\boldsymbol{\varepsilon} \sim N_n(\mathbf{0}, \sigma^2\Lambda)$. When Λ is the $n \times n$ identity matrix then we are back to the case of independent and identically distributed random errors. More generally, Λ will be parametrized by a vector $\boldsymbol{\theta}$: $\Lambda(\boldsymbol{\theta})$.

Now, let Θ denote the set of all model parameters except σ^2. The concentration will be

model as a parametric function of Θ. Thus the likelihood portion of our model is

$$\ln(Y_j) \mid \Theta \sim N[C(t_j), \sigma^2]. \tag{2}$$

(Note that we refer to the true concentration as $C(t)$ and our model, presented below, of the true concentration also as $C(t)$. Although the model depends on Θ, we do not explicitly show this dependence.)

2.2 The concentration, $C(\cdot)$

We assume a convolution model for hormone concentration. A goal then is to deconvolve the concentration into a secretion function and a clearance function. The first order, linear differential equation (with initial condition)

$$\frac{dC(t)}{dt} = kC(t) + S(t); \quad C(0) = C_0,\, k > 0 \tag{3}$$

is the starting point for deconvolution methods. The equation states that the change in hormone serum concentration at time t is proportional to both the concentration and the amount of hormone secreted, $S(t)$, at time t. This equation is easily solved by introducing the integrating factor $\exp(\int_0^t k\,dx) = \exp(kt)$. The solution to (3) is

$$C(t) = C_0 \exp(-kt) + \int_0^t S(x) \exp[k(x-t)]dx \tag{4}$$

for $k > 0$ where the integral on the right hand side (rhs) is the convolution integral of the hormone secretion with exponential decay (the clearance function).

Denote the secretion rate by $S(t)$, which can be written as the sum of the basal secretion (the underlying oscillatory component), $B(t)$, and the pulsatile secretion, $P(t)$: $S(t) = B(t) + P(t)$. Furthermore, there may exist microscopic biologic fluctuation in secretion that we represent by $G(t)$. (4) can be extended to include this variation (Keenan, Veldhuis, and

Yang, 1998):

$$\begin{aligned} C(t) &= C_0 \exp(-kt) + \int_0^t [G(x) + B(x) + P(x)] \exp[k(x-t)]dx \\ &= \underbrace{C_0 \exp(-kt) + \int_0^t [G(x) + B(x)] \exp[k(x-t)]dx}_{F(t)} + \int_0^t P(x) \exp[k(x-t)]dx \\ &= F(t) + \int_0^t P(x) \exp[k(x-t)]dx. \end{aligned}$$

$C(\cdot)$ will be completely specified after we define $F(\cdot)$ and $P(\cdot)$. Often, the main interest lies in the number of pulsatile secretion events and the amount of hormone secreted during each event. Thus we consider $F(\cdot)$ a nuisance.

2.2.1 The nuisance function, $F(\cdot)$

$F(\cdot)$ is the summation of the initial concentration times exponential decay, the microscopic biologic variation in concentration and the convolution of the basal secretion with the exponential decay. We believe that $F(\cdot)$ should vary smoothly over time and put no further restrictions on it. We model it with a b-spline (de Boor, 1978) function with an unknown number of knots with unspecified locations. We estimate the number and locations of the knots as well as the spline coefficients. Johnson (2003) considers a similar model for the concentration, however he only considers a constant function $F(t) \equiv c$. Here, we consider a more general form for $F(\cdot)$ by modeling it with a cubic b-spline. In particular, let N_K denote the number of interior knots at locations $\{\xi_i\}_{i=1}^{N_K}$ (throughout this manuscript, we drop the indices on sets after their initial definition). We consider both N_K and $\{\xi_i\}$ to be unknown quantities that are to be estimated. Further, conditional on N_K let $\{\beta_i\}_{i=1}^{(N_K+4)}$ denote the set of b-spine coefficients and $X(\{\xi_i\})$ a design matrix whose rows are the basis functions for the b-spline represention of the function $F(\cdot)$. Note that X depends on both the number and location of the knots. For notational clarity, we ignore the dependence of X on the number and location of the knots. The dimension of X is $N \times (N_K + 4)$ where N is the number of observations. Note that 8 additional knots (in addition to the interior knots) must be specified for a cubic b-spline. We place the first four knots at 0, the beginning of the data,

and the last four knots at T, the end of the data collection period. We take time $t = 0$ to denote the beginning of the data collection period. Then $F(\cdot)$ can be approximated at the observation times t_j by

$$F(t_j) = \langle X^{\mathrm{T}}_{j,\cdot}\,,\, \boldsymbol{\beta}_{N_K} \rangle$$

where $X^{\mathrm{T}}_{j,\cdot}$ is the jth row of X and $\boldsymbol{\beta}_{N_K} = (\beta_1, \ldots, \beta_{N_K+4})^{\mathrm{T}}$ and $\langle x,\, y \rangle$ is the inner product of the vectors x and y. Next, we define the pulsatile secretion function.

2.2.2 The pulsatile secretion function, $P(\cdot)$

Parallel to the development in O'Sullivan and O'Sullivan (1988), we assume that the signaling of the release of hormone can be modeled by a point process $\{\tau_i\}_{i\geq 1}$ and its associated counting function $N((a,b]) = \sum_{i\geq 1} I_{(a,b]}(\tau_i)$. We generalize their development by attaching marks, $\{\boldsymbol{\gamma}_i\}_{i\geq 1}$, to the process $\{\tau_i\}$ in a measurable marking space $(\mathcal{M}, \mathcal{F})$ with probability measure μ. We will further assume that μ is absolutely continuous with associated density $f(\boldsymbol{\gamma} \mid t)$. Then, $\{\tau_i, \boldsymbol{\gamma}_i\}_{i\geq 1}$ is, in its own right, a point process with associated counting function: $N((a,b] \times A) = \sum_{i\geq 1} I_{(a,b]\times A}(\tau_i, \boldsymbol{\gamma}_i)$ where $A \in \mathcal{F}$. Let $\lambda(t)$ denote the (marginal) rate function of $\{\tau_i\}$. Then the rate function of $\{\tau_i, \boldsymbol{\gamma}_i\}$ is $\lambda(t) f(\boldsymbol{\gamma} \mid t)$. Further, let $p(t;\, \boldsymbol{\gamma})$ represent a family of non-negative functions parametrized by $\boldsymbol{\gamma}$. The pulsatile component, $P(\cdot)$, of the secretion function is given by the convolution of $p(t, \boldsymbol{\gamma})$ and $N((a,b] \times A)$:

$$\begin{aligned} P(t) &= \int_{(\nu,\, y)\in(0,t]\times A} p(t-\nu;\, \boldsymbol{\gamma} - \mathbf{y}) dN((\nu,\, \mathbf{y})) \\ &\stackrel{\text{def}}{=} \sum_{i\geq 1} p(t-\tau_i;\, \boldsymbol{\gamma}_i) I_{(0,t]\times A}(\tau_i,\, \boldsymbol{\gamma}_i) \\ &= \sum_{i=1}^{N(t)} p(t-\tau_i;\, \boldsymbol{\gamma}_i) \end{aligned} \tag{5}$$

where $t \in (0, T]$ is the observation interval of the experiment.

The pulse functions, $p(t; \boldsymbol{\gamma})$, are taken to be Gaussian shaped in this manuscript:

$$p(t; \boldsymbol{\gamma}) = \alpha \exp(-0.5t^2/\nu^2)/\sqrt{2\pi\nu^2}.$$

where $\boldsymbol{\gamma} = (\alpha, \nu^2)$, α represents the amount of hormone secreted by a gland due to the signal

at time τ_i and ν^2 controls the width of the function $p(t;\boldsymbol{\gamma})$. Thus $\mathcal{M} = \mathbb{R}^+ \times \mathbb{R}^+$ and $\mathcal{F}$ are the Lebesque measurable rectangles in $\mathcal{M}$.

Remark 1: We are taking a bit of notational liberty here. The process $\{\tau_i\}$ represents both the signaling mechanism arrival times and the arrival times of the centers of the Gaussian-shaped pulse functions $p(t-\tau_i;,\boldsymbol{\gamma}_i)$; implying that the gland releases $\alpha_i/2$ hormone prior to the signal. Technically, the signal should precede any hormone secretion. This would be the case if $p(t;\boldsymbol{\gamma}) \propto \alpha t^{\gamma-1}\exp(-\beta t)$ with $\boldsymbol{\gamma} = (\alpha,\beta,\gamma)$ for $t \geq 0$. In fact, within the Bayesian framework, the pulse function family can be virtually any non-negative family of functions. Henceforth, the process $\{\tau_i\}$ will represent the arrival times of (the centers of) the pulse functions $p(t-\tau_i;\boldsymbol{\gamma}_i)$ with the understanding the the signaling mechanism precedes any (significant amount of) hormone release: $\int_{-\infty}^{s_i} p(t-\tau_i;\boldsymbol{\gamma}) \approx 0$, where $s_i(\leq \tau_i)$ is the ith signaling event.

Remark 2: Marking the process allows for biological variation in the amount of hormone released during each pulse event. This biological variation may be due to several factors including the strength of the signaling mechanism and the amount of hormone in the gland available for secretion among other factors such as known or unknown positive and negative feedback mechanisms.

Remark 3: Allowing the process to have a nonhomogeneous rate function gives flexibility in modeling the shape and size of a *pulsatile secretion event* (loosely defined as a large quantity of hormone released in a relatively short period of time). It also allows for alternating active and quiescent periods of hormone release throughout the day. Thus, a pulsatile secretion event may consist of a single pulse function pulse $p(t-\tau_i;\boldsymbol{\gamma}_i)$ or of the superposition of several pulse functions derived from a rapid succession of signals.

The last piece needed to complete the specification of $C(\cdot)$ is the elimination function.

2.2.3 The elimination function

There are several mechanisms for the elimination of hormone from the circulatory system including specific target cite binding, enzymatic cleavage and glomerular filtration. Typically these mechanisms cannot be modeled individually and a single elimination function is used to model the overall clearance rate. This elimination function that describes the removal of hormone from the circulatory system, is typically chosen to be exponential or bi-exponential decay unless experimentation suggests some other form. In this manuscript we will assume that clearance is exponential: $\exp(-kt)$. We model the half-life of the clearance function: $t_{1/2} = \ln(2)/k$, instead of the decay rate, k, which helps with convergence properties of the MCMC simulation.

2.3 Parameter priors

2.3.1 Prior factorization

We factor the joint prior as

$$
\begin{aligned}
&\pi\left[\{\beta_i\}, \beta, \psi^2, \{\xi_i\}, N_K, \{\tau_j\}, \{\nu_j^2\}, \nu, \zeta^2, \{\alpha_j\}, \alpha, \phi^2, N(T), t_{1/2}, \sigma^2\right] \\
&= \prod_{i=1}^{N_K} \left[\pi(\{\beta_i\} \mid N_K, \beta, \psi^2)\, \pi(\{\xi_i\} \mid N_K)\right]\, \pi(N_k)\, \pi(\beta)\, \pi(\psi^2) \qquad (6) \\
&\times \left\{ \prod_{j=1}^{N(T)} \left[\pi(\tau_j \mid N(T))\, \pi(\alpha_j \mid N(T), \alpha, \phi^2)\, \pi(\nu_j^2 \mid N(T), \nu, \zeta^2)\right] \right. \\
&\qquad \left. \pi(N(T))\, \pi(\nu)\, \pi(\zeta^2)\, \pi(\alpha)\, \pi(\phi^2) \right\} \qquad (7) \\
&\times \pi(t_{1/2})\, \pi(\sigma^2). \qquad (8)
\end{aligned}
$$

(6) includes priors for parameters of the nuisance function, $F(\cdot)$, as well as hyperpriors on these parameters; (7) are the priors (and hyperpriors) for the parameters of the pulsatile secretion function, $P(t)$; and (8) is the product of the prior for the half-life of the clearance function and the model variance σ^2.

2.3.2 Priors for the parametrized function $F(\cdot)$

The number of knots, N_K, is assigned a Negative Binomial prior with mean 3 and variance 6: $N_k \sim Negbin(3, .5)$. The number of knots can be thought of as a smoothing parameter in a b-spline representation (de Boor, 1978) with fewer knots resulting in a smoother function $F(\cdot)$. Since we believe that $F(\cdot)$ should be a rather smooth function (fewer oscillations), we chose to assign N_K a Negative Binomial prior with a small mean. Conditional on N_K, the a knots locations $\{\xi_i\}$ are a-priori distributed as N_K independent, uniform random variables over the time period of data collection: $[0, T]$. Their conditional joint prior density is thus $p(\xi_1, \ldots, \xi_{N_K} \mid N_K) = T^{-N_K}$.

The last set of parameters that require a prior, for the specification of $F(\cdot)$, is $\{\beta_i\}$. $F(\cdot)$ is necessarily a non-negative function. Since the basis functions of the b-spline representation are non-negative, a sufficient condition for a b-spline function to be non-negative is that each b-spline coefficient β_i, $i = 1, \ldots, N_K$ be non-negative (de Boor, 1978). Therefore, we model the natural log of the b-spline coefficients hierarchically: $\ln(\beta_i) \mid N_K, \beta, \psi^2 \sim N(\beta, \psi^2)$ with $\beta \sim N(3, 1)$ and $\psi^2 \sim IG(2.1, 2)$, the inverse gamma function.

2.3.3 Priors for the parametrized function $P(\cdot)$

Next, we specify the priors necessary for the pulsatile component of the secretion $P(\cdot)$ in (5). The priors are specified hierarchically. We begin with the number of pulse functions, $N(T)$. We will assume a-priori that the stochastic process, $\{\tau_i\}$, governing the arrival times of the pulse functions is a homogeneous conditional Poisson process, given λ, with intensity $\lambda^* = \lambda/T$ (any indications of a nonhomogeous process that are present in the data will be reflected in the posterior). We reflect uncertainty in λ by placing a prior distribution on it as well: $\lambda \mid a_\lambda, b_\lambda \sim G(a_\lambda, b_\lambda)$. Then $N(T) \mid \lambda^* \sim Pois(\lambda)$. For a homogeneous Poisson process, $\{\tau_i\}$, it is well known that the joint distribution of $\tau_1, \ldots, \tau_{N(T)}$ given $N(T) = n$ is distributed as the order statistics from n independent and identically distributed uniform random variables with support $[0, T]$: $\pi(\tau_1, \ldots, \tau_{N(T)} \mid N(T) = n) = n!/T^n$.

Conditional on $N(T)$, the remaining parameters are $(\boldsymbol{\gamma}_1, \ldots, \boldsymbol{\gamma}_{N(T)})$. Recall that $\boldsymbol{\gamma}_i = (\alpha_i, \nu_i^2)$. We assume a-priori that these parameters are independent of the arrival times of the events. We also assume that elements of the set $\{\alpha_i\}$ are a-priori conditionally independent and the elements of the set $\{\nu_i^2\}$ are a-priori conditionally independent and that α_i iand ν_j^2 are independent for all i and j. We specify prior of ν_i^2 hierarchically on the log scale:

$$\begin{aligned} \ln(\nu_i^2) \mid \nu, \zeta &\overset{\text{iid}}{\sim} N(\ln(\nu), \zeta^2), \quad i = 1, \ldots, N(T) \\ \ln(\nu) &\sim N(m_\nu, v_\nu^2) \\ \zeta^2 &\sim IG(a_\zeta, b_\zeta). \end{aligned}$$

The amount of hormone secreted from pulse function i, namely α_i is also strictly positive. We specify its prior hierarchically:

$$\begin{aligned} \ln(\alpha_i) \mid \alpha, \phi &\overset{\text{iid}}{\sim} N(\ln(\alpha), \phi^2), \quad i = 1, \ldots, N(T) \\ \ln(\alpha) &\sim N(m_\alpha, v_\alpha^2) \\ \phi^2 &\sim IG(a_\phi, b_\phi). \end{aligned}$$

We believe that there may be biological variation from pulse to pulse, however, we also believe that the pulse functions should be more or less similar. Modeling these pulse function shape parameters hierarchically reflects this believe. Note that this hierarchical modeling also reduces the influence of the priors on the posterior estimates.

The hyperpriors a_λ, b_λ, a_ζ, b_ζ, a_ϕ, b_ϕ, m_ν, v_ν^2 and m_α, v_α^2 are all constant and depend on the particular hormone under investigation.

2.3.4 Priors for $t_{1/2}$ and σ^2

The last two parameters that require prior specifications are the half-life, $t_{1/2}$, and the model variance, σ^2. We choose to model the decay function in terms of the hormone half-life instead of the decay rate, k. During MCMC simulation of the posterior, we found that modeling hormone clearance from the system in terms of the half-life resulted in better simulation performance. When the decay rate was used, it often happened that both it and

the $\{\alpha_i\}$ would simultaneously escape to very large numbers, numbers that are biologically impossible, never to return. This is easy to control with a suitable prior under the half-life parametrization because as $k \to \infty$, $t_{1/2} \to 0$. Since the half-life is a strictly positive number we assign it a log-normal prior: $\ln(t_{1/2}) \sim N(m_t, v_t)$. The prior mean and variance will depend on the particular hormone under investigation. The model variance is given a vague, proper prior: $\sigma^2 \sim IG(0.001, 0.001)$.

3 Simulating from the posterior

The full joint posterior is not analytic in form. Thus we resort to MCMC simulation of the posterior distribution. Furthermore, the number and location of both the b-spline knots as well as the number and location of the pulse function arrival times (and associated marks) are unknown. Standard MCMC techniques are not equipped to handle variable-dimension parameter space problems. Recent advances in Bayesian computation, however, have made varaible-dimension problems feasible. We use the birth-death Markov Chain Monte Carlo (BDMCMC) algorithm developed by Stephens (2000) to simulate the number of spline knots, their locations and the spline function parameters. A separate BDMCMC algorithm is used to draw the number of pulse functions $N(T)$, their locations and associated marks. Both BDMCMC algorithms are imbedded within the MCMC simulation of the remaining parameters. An alternative algorithm to the BDMCMC algorithm that could also be used is the reversible-jump MCMC algorithm due to Green (1995)

The BDMCMC requires exchangeable priors and likelihoods (Stephens, 2000). The conditional prior $\pi(\tau_1, \ldots, \tau_{N(T)} \mid N(T))$ violates this requirement. Thus to implement the BDMCMC alogirthm on the pulse function parameters, we further condition on a random permutation of the arrival time indices $(1, \ldots, N(T))$. Let p denote this random permutation with conditional prior $\pi(p \mid N(T)) = 1/N(T)!$. We then have

$$\pi(\tau_{p(1)}, \ldots, \tau_{p(N(T))} \mid N(T)) = \pi(\tau_1, \ldots, \tau_{N(T)} \mid N(T)\, \pi(p \mid N(T)) = T^{-N(T)}$$

and it is this joint distribution of the arrival times and a random permutation of those times

conditional on $N(T)$ that is used in the BDMCMC algorithm. As for the $\{\alpha_i\}$ and $\{\nu_i^2\}$, they are all a-priori independent. At the end of the simulation, we can easily convert back to the ordered arrival times. As an aid to chain mixing, after the BDMCMC algorithms return to the main MCMC chain, the parameters drawn from the BDMCMC algorithm are further updated with standard Gibbs or Metropolis-Hastings steps as suggested by Stephens (2000).

Remark 4: This permutation of the arrival times is justified by the fact that the simplest way to simulate the arrival times of a Poisson process with intensity λ in an interval $(a, b]$ conditional on $N((a, b])$ is to 1) draw $N((a, b])$ from a Poisson distribution with mean $\lambda(b - a)$; 2) draw $N((a, b])$ independent uniform random variables on $(a, b]$; and 3) order them. Conceptually, the BDMCMC algorithm executes 1) and 2).

4 Example

We now apply the BDM to a randomly selected cortisol data set from the study described in the introduction. The time series is shown in the upper-left panel of Figure 1. The data collection takes place over a 24 hour period. Thus $T = 24$. To begin we specify our priors and hyperpriors for the pulse function parameters and the half-life: $\alpha_\lambda = 10$ and $\beta_\lambda = 1$. Thus, $\lambda \mid \alpha_\lambda, \beta_\lambda \sim G(10, 1)$ and reflects our believe that the number of secretion events should be about 10 in a 24 hour period and thus, a-priori we believe that each secretion event should be made up of 1 pulse function. However, it is also variable enough to allow fewer events and allow for the possibility that secretion events may be made up of several component functions. For the amount of hormone released, we set $m_\alpha = 3$, $v_\alpha^2 = 1$, $a_\phi = 5$ and $b_\phi = 2$. For the "width" of the pulse functions we set $m_\nu = -1$, $v_\nu^2 = 1$, $a_\zeta = 5$ and $b_\zeta = 2$. For the half-life we have $\ln(t_{1/2}) \sim N(-1, 1)$. Upon exponentiating, this prior has 90% of its mass between 0.07 and 1.9. Only 1.6×10^{-4} of the mass is less than 0.01, thus controlling the half-life from getting too small (cortisol half-lives are typically from 30-60 minutes).

We ran the MCMC simulation for 225,000 iterations with a burn-in of 25,000. The chain

was thinned by saving every 100th sample. The simulation took 19 minutes on a 2.7 GHz Power Mac G5. Convergence was assessed graphically on the parameters that are fixed-dimension. Good mixing was realized for both BDMCMC algorithms with N_K taking on a different value approximately 4% of the time and $N(T)$ taking on a different value roughly 10% of the time.

Graphical results are given in Figure 1. The upper-right panel of Figure 1 shows the expected value of the posterior predictive density (PPD) of the concentration (dark blue) as well as the 95% point-wise credible bounds of the PPD (light blue). The lower-left panel shows the posterior mean of the nuisance function $F(t) \mid Y$ (dark blue) as well as the 95% point-wise credible bounds (light blue). The posterior estimated mean of the pulsatile secretion function $P(t)$ and 95% point-wise credible bounds are displayed in the lower-right panel. Fits were obtained by marginalizing the posterior over N_K and $N(T)$.

Overall, the model fits the data well. Figure 2 show both the Bayesian deleted residuals (Gelfand, Dey, and Chang, 1992) and the autocorrelation function of those residuals. Overall, the residuals show no structural pattern, indicating that the mean structure of the data has been captured by the model. There are only one or two outliers (absolute residual value greater than 3). Furthermore, it appears that the assumption of independent errors is justified by the autocorrelation function of the residuals. Although time series data typically display autocorrelation, once the mean structure has been accounted for in this example, no correlation remains. Even if biological error is correlated, the assay error most likely dominates it. It is reasonable to assume that assay error is independent. Further evidence of model fit was ascertained by computing a Bayesian good-of-fit statisitic (Johnson, 2004). The value of the statistic was 0.502. Under the null hypothesis that the model fits well, a value of 0.5 is expected.

5 Estimating the posterior rate function

The number and location of secretion events are often of interest to the investigator. The posterior mean of the pulsatile secretion function, shown in the lower right panel of Figure 1, and the 95% point-wise credible bounds give a good indication of the locations of these events and an indication of how likely it is that a secretion event occurs in a given interval of time. However, two question often asked are:

1. What is the probability that a secretion event occurs at time t?

2. How many secretion events are there?

This figure does not go far enough in addressing these questions.

Johnson (2003) allocates pulse functions to secretion events by considering any group of pulse functions whose superposition results in a function with a single global maximum as a single secretion event. The resulting posterior distributions of the number of secretion events on the data sets he considers all have a dominant mode. That mode is taken as the number of secretion events. No estimate of the probability that something is an event was attempted, nor was it necessary. For the cortisol data set we consider in this manuscript, this method is unsatisfactory. A dominant secretion event mode does not exist; the mode occurs only 18% of the time (not shown). Furthermore, we want to estimate the posterior probability that a secretion event occurs in an arbitrary interval. Johnson (2003) did not address this issue. Furthermore, his definition of a secretion event is rather arbitrary.

We propose a different solution that answers both questions without a formal definition of a secretion event: The procedure consist of the follow three steps:

1. Estimate the marginal posterior rate function $\lambda^*(t) \mid Y$ of the posterior process $\{\tau_i\} \mid Y$.

2. Estimate the location of secretion event j, SE_j, as the jth ordered local maximum, M_j of $\lambda^*(t) \mid Y$.

3. For a neighborhood, $\mathcal{M}_j$, containing M_j: $M_j \in \mathcal{M}_j$, estimate the probability that at least one pulse arrival time is contained in $\mathcal{M}_j$. Take this estimate as the probability that SE_j occurs in $\mathcal{M}_j$.

Step 1: Define the posterior rate function, $\lambda^*(t) \mid Y$, implicitly by $E(N(t) \mid Y) = \int_0^t \lambda^*(s) \mid Y\, ds$ for $t \in [0,T]$. Suppose $\lambda^*(t) \mid Y$ is bounded and continuous on $[0,T]$. Then

$$\lim_{h\to 0} \frac{1}{h} E[N(t+h) - N(t) \mid Y] = \lim_{h\to 0} \frac{1}{h} \int_t^{t+h} \lambda^*(s) \mid Y ds = \lambda^*(t) \mid Y.$$

This suggests a way to estimate $\lambda^*(t) \mid Y$. Partition $[0,T]$ into n subintervals $A_i = (t_{i-1}, t_i]$, $i = 1, \ldots, n$, $t_0 = 0$, $t_n = T$ each of length T/n. Then

$$\lambda^*(t_i) \mid Y \approx \frac{n}{T} E[N(t_i) - N(t_{i-1}) \mid Y], \quad i = 1, \ldots, n.$$

The expectation can be approximated from the MCMC posterior samples. Suppose we save $\mathcal{S}$ of them. Then

$$E[N(t_i) - N(t_{i-1}) \mid Y] \approx \frac{1}{\mathcal{S}} \sum_{j=1}^{\mathcal{S}} \sum_{k=1}^{N(T)^{(j)}} I_{A_i}(\tau_k^{(j)}), \quad i = 1, \ldots, n \tag{9}$$

where the superscript (j) indicates parameter values from the jth MCMC sample. The rhs of (9) is a histogram estimate of the counts of $\{\tau_{p(i)}\} \mid Y$. We wish to have a smooth estimate of $\lambda^*(t) \mid Y$ and thus seek a smooth estimate of the histogram.

Consider the marginal posterior density

$$\pi(\{\tau_{p(i)}\} \mid Y) = \sum_{k=0}^{\infty} \pi(\{\tau_{p(i)}\} \mid N(T) = k, Y) \pi(N(T) = k \mid Y). \tag{10}$$

This can be estimated by dividing the rhs of (9) by $\sum_{j=1}^{\mathcal{S}} N(T)^{(j)}$. Therefore, $\lambda^*(t) \mid Y$ is proportional to this marginal posterior density. Thus, by estimating the marginal density, we estimate $\lambda^*(t) \mid Y$. We estimate this density with a mixture of normal density components whose number is unknown. We choose a Bayesian model for density estimation using mixtures of Dirichlet processes (MDP, Ferguson, 1973; Antoniak, 1974; MacEachern and Müller, 1998) that was first proposed by Escobar and West (1995).

The MDP model is as follows. The data are the marginal posterior draws of the τ_j. The dependence on Y and on the permutation p is dropped only for notational convenience. Each observation is allowed it's own set of parameters. The parameters are assumed to be distributed, iid, according to a distribution G, with additional uncertainty about the prior distribution G. In particular, G is a random distribution generated by a Dirichlet process with base measure $\alpha_0 N(\mu, \sigma^2)$ and total mass parameter α_0:

$$\begin{aligned} \tau_j &\sim N(\mu_j, \sigma_j^2) \\ (\mu_j, \sigma_j^2) &\sim G \\ G &\sim DP[(\alpha_0, N(\mu, \sigma^2)]. \end{aligned}$$

We also place priors on the parameters of the base measure in the Dirichlet process:

$$\mu \sim U(0, T), \quad \sigma^2 \sim IG(2.1, \beta), \quad \alpha_0 \sim G(1, 1)$$

with hyperprior $\beta \sim G(1, 1)$. The estimation of this model follows that given by Neal (2000). We estimate the posterior of α_0 by the method proposed in Escobar and West (1995). Let $\hat{\lambda}^*(t) \mid Y$ denote the estimated marginal posterior rate function. It is shown by the red curve in Figure 3. The gray region under the curve is the histogram based estimate of $\lambda^*(t) \mid Y$.

Step 2: The arrows at the bottom of the Figure 3 show where all local maxima, M_j, $j = 1, \ldots, 34$, occur for the data set analyzed above (some of which are so small that they are not visible in $\hat{\lambda}^*(t) \mid Y$). These local maxima are take to be point estimates of locations of the secretion events SE_j, $j = 1, \ldots, 34$. These maxima are easily obtained since the mixture density is a mixture of normal density components. We can easily estimate the expected first and second derivatives of $\hat{\lambda}^*(t) \mid Y$ on a fine grid of $[0, T]$ during the MCMC simulation of the MDP model and numerically estimate where the first derivative equals zero and the second derivative is negative.

Step 3: For any given interval, $\mathcal{I} \subset [0, T]$, it is easy to estimate the posterior expected number of pulse arrivals in $\mathcal{I}$:

$$E[N(\mathcal{I}) \mid Y] \approx \int_{\mathcal{I}} (\hat{\lambda}^*(t) \mid Y) dt. \tag{11}$$

The integral can be approximated numerically. Also the posterior probability that at least one pulse arrival occurs in $\mathcal{I}$ is easily estimated:

$$\Pr[N(\mathcal{I}) \mid Y \geq 1] \approx \frac{1}{\mathcal{S}} \sum_{j=1}^{\mathcal{S}} I(N(\mathcal{I})^{(j)} \geq 1) \tag{12}$$

For certain intervals $\mathcal{I}$ that contain M_j, $j = 1, \ldots, J$, this probability can be taken to be the probability that SE_j takes place in $\mathcal{I}$. To automate this procedure, define m_j as the jth local minima of $\lambda^*(t) \mid Y$ (also easily approximated on $\hat{\lambda}^*(t) \mid Y$). Define $m_0 = 0$ and $m_{J+1} = T$. Further, let $\mathcal{I}_j = (m_{j-1}, m_j]$, $j = 1, \ldots, J$. Now (11) and (12) can be estimated for each of the intervals $\mathcal{I}_j$.

The probabilities (12) for intervals $\mathcal{I}_j$, $j = 1, \ldots, 34$, are shown in the bottom half of Figure 3 for the data set examined in Section 4. The blue lines denote the locations M_j, $j = 1, \ldots, J$ of the secretion events. The heights of the lines indicates the probabilities. The rug at the bottom of Figure 3 denote the local minima. Further, we find that $E[N(24) \mid Y] \approx 14.70$ while the expected number of secretion events is $\sum_{j=1}^{34} \Pr[N(\mathcal{I}_j) \mid Y \geq 1] \approx 12.67$.

We also compare the fit of our model with the recent model/method proposed by Yang, Liu, and Wang (In Press). They model pulsatile hormone data with a non-linear mixed effects partial spline model (NMPSM). Figure 4 displays fits from both models (blue—BDM, red—NMPSM). There are several notable differences. First, around 9:00 p.m. the BDM finds (based on thresholding the probabilities at 0.75) two "secretion events" that are not fit with the NMPSM. There is one other "event", around 4:30 a.m. that is found by BDM and not by the NMPSM. The NMPSM has no chance of selecting the two around 9:00 p.m. as it relies on an initial guess of where events occur. The heuristic procedure used to initialize event locations did not identify these two as events. The "event" at 4:30 a.m. was identified by the heuristic procedure as a potential event. After the NMPSM is fit to the data, one of GCV, RIC, AIC or BIC criteria is used to select the final number of events. Yang, Liu, and Wang (In Press) recommends BIC. We chose BIC here, which did not select this event. The other difference with respect to events is the location of the "event" just prior to 3:00 p.m. The BDM and the NMPSM finds different locations for it. Note that the arrows at

the bottom of this figure show point estimates of event locations. The BDM point estimates always precede those of NMPSM. This is due to the fact the the BDM point estimate is for the secretion event location and the NMPSM point estimate is the MLE of the center of the pulse wave-form for the concentration (the convolution of secretion and elimination). As to what is the truth in this data set, we do not know. This comparison demonstrates what we said in the introduction. Models that rely on initial estimates of the number and location of events cannot recover from missed events.

6 Comparison of Error Structures

Although no residual correlation was found in the example presented, one may still question the assumption of independent errors for time series data. Thus to investigate this assumption, we analyze all 52 cortisol data sets using five different error structures and two slight model modifications. Models are compared using Bayes factors (Gelman et al., 1997; Robert, 2001). The first model is that described in Section 2. The next three models also assume independent errors. However, for the second model we add one to the observed concentration prior to the log transformation. (The rationale here is that some data sets have observed concentrations that range from near zero to about 5-10. The log-transformed time series turns out to be 'V' shaped that makes it difficult to model $F(t)$ with a spline). The third models the time series on the natural scale. For the fourth model, we model a constant coefficient of variation, allowing the error variance to depend on the mean (as does the log Normal model) and analyze the data on its natural scale. An AR1 error structure is assumed for the last three models. These three models introduced correlation between the error terms. The correlation between ε_i and ε_j is $\rho^{|i-j|}$. We further assume that this correlation is non-negative and place a $U[0,1]$ prior on it. The models are tabulated below.

Overall, the second model fits best; however only slightly better than model 4. In terms of Bayes factors, the data support it in favor of the other models in 23 of the 52 data sets. The second best fitting model is the constant CV model where the data favored it in 18 of

Table 1: Comparison of various models and error structures. The forth column is the number of data sets that each model fit best, according to the estimated Bayes factors. The last column tabulates the average Bayes factor (over all 52 data sets) relative to model 2.

Error Structure	Model	Data	Best	$10\log_{10}(\overline{BF})$
Independent	log Normal	Y	6	13.84
Independent	log Normal	$Y+1$	23	0.00
Independent	Normal	Y	5	63.21
Constant CV	Normal	Y	18	4.78
AR1	log Normal	Y	0	164.89
AR1	log Normal	$Y+1$	0	146.43
AR1	Normal	Y	0	182.42

the 52 data sets. The last column of the Table 1 tabulates the the average Bayes factor over all 52 data sets relative to model 2. The Bayes factors are transformed to the log-base-10 scale and multiplied by 10. On this scale, a Bayes factor of 0-5 indicates that the data slightly favor, perhaps not worth mentioning, model 2 over the competing model. A value of 5-11 indicates the data favor model 2 over the competing model. A value of 11-22 indicates strong evidence in the data for model 2 versus the competing model and a value of > 22 indicates very strong evidence for model 2.

These results suggest that the two models, model 2 and 4, where the error variance is a function of the mean concentration fit best. The AR1 error structure is evidently not appropriate for these data. In fact, model 2 was used in the example given in Section 4.

7 Discussion

Our method extends earlier work by Johnson (2003) in two significant aspects. First, we allow for a non-constant basal concentration. Second, we estimate probabilities of secretion events. We also extend the work by O'Sullivan and O'Sullivan (1988) in that we convolve a marked point-process with pulse functions at the secretion level (they convolve a point-process with a function that represents the shape of a pulse at the level of hormone concentration). This convolution is further convolved with an elimination function that results in hormone

concentration. By marking the point-process, we allow for biological variation in the size and shape of each pulse function. Lastly, O'Sullivan and O'Sullivan (1988) assume a zero basal concentration; we allow the basal concentration to be an arbitrary function that is approximated by a spline function. Our method also generalizes that of Yang, Liu, and Wang (In Press) in that the BDM does not rely on an ad-hoc method to initialize the number and location of events.

The BDM can easily incorporate other pulse function forms, such as a Laplacian or Gamma, further any form of the elimination function is possible. The only technical difficulty may be in the convolution of these two functions as it may not have an analytic solution. The convolution of a Gaussian and exponential decay does not have an analytic solution, but is proportional to the error function, erf, which can be efficiently computed (see Johnson (2003)). Alternatively, one can use the Fourier transform to compute the convolution in the frequency domain and transform the result back to the time domain.

Disadvantages of the BDM approach is that is it rather difficult to elicit prior information and to implement the advanced MCMC simulation (code is available from the first author). Further, because of the ill-posed nature of the deconvolution problem (Wahba, 1990), uninformative prior specification and an objective Bayesian approach may not be feasible. Lastly, the Bayesian approach is computationally intensive. The MCMC simulation of the cortisol data set takes about 19 minutes on a dual 2.7 GHz PowerPC G5. Further the MDP post-processing takes an additional 15 minutes.

Acknowledgements

The author would like to thank Dr. Elizabeth A. Young of the Department of Psychiatry and Mental Health Research Instisute, University of Michigan, for the use of the cortisol hormone data. I also thank Professor Yuedong Wang, Department of Applied Probability and Statistics, Univeristy of California, Santa Barbara, for analyzing the data set with NMPSM. Thanks also to Professor Thomas Braun, Deparment of Biostatistics, University

of Michigan for his helpful comments. This work was funded by the NIH, grant number P60 DK20572.

References

Antoniak, C. E. (1974). Mixtures of Dirichlet processes with applications to Bayesian nonparametric problems. *The Annals of Statistics* **2**, 1152–1174.

Berne, R. M. and Levy, M. N., editors (1993). *Physiology*. 3rd edition. St. Louis, MO: Mosby Year Book.

de Boor, C. (1978). *A Practical Guide to Splines*. New York: Springer-Verlag.

Diggle, P. J. and Zeger, S. L. (1989). A non-Gaussian model for time series with pulses. *Journal of the American Statistical Association* **84**, 354–359.

Escobar, M. D. and West, M. (1995). Bayesian density estimation and inference using mixtures. *Journal of the American Statistical Association* **90**, 577–588.

Ferguson, T. S. (1973). A Bayesian analysis of some nonparametric problems. *The Annals of Statistics* **1**, 209–230.

Gelfand, A. E., Dey, D. K., and Chang, H. (1992). Model determination using predictive distributions and implementation via sampling-base methods (with discussion). In Bernardo, J. M., et al., editors, *Bayesian Statistics 4*, pages 147–167. Oxford: Oxford University Press.

Gelman, A., et al. (1997). *Bayesian Data Analysis*. New York: Chapman & Hall.

Green, P. J. (1995). Reversible jump Markov chain Monte Carlo computation and Bayesian model determination. *Biometrika* **82**, 711–732.

Guo, W., Wang, Y., and Brown, M. B. (1999). A signal extraction approach to modeling hormone time series with pulses and a changing baseline. *Journal of the American Statistical Association* **94**, 746–756.

Johnson, T. D. (2003). Bayesian deconvolution analysis of hormone concentration profiles. *Biometrics* **59**, 650–660.

Johnson, V. E. (2004). A Bayesian chi-squared test for goodness of fit. *Annals of Statistics* **32**, 2361–2384.

Keenan, D. M. and Veldhuis, J. D. (2003). Cortisol feedback state governs adrenocorticotropin secretory-burst shapes, frequency, and mass in a dual-waveform construct: Time of day-dependent regulation. *American Journal of Physiology* **285**, R950–R961.

Keenan, D. M., Veldhuis, J. D., and Yang, R. (1998). Joint recovery of pulsatile and basal hormone secretion by stochastic nonlinear random-effects analysis. *American Journal of Physiology* **275**, R1939–R1949.

Komaki, F. (1993). State-space modelling of time series sampled from continuous processes with pulses. *Biometrika* **80**, 417–429.

Kushler, R. H. and Brown, M. B. (1991). A model for the identification of hormone pulses. *Statistics in Medicine* **10**, 329–340.

MacEachern, S. N. and Müller, P. (1998). Estimating mixtures of Dirichlet process models. *Journal of Computational and Graphical Statistics* **7**, 223–238.

Mauger, D. T. and Brown, M. B. (1995). A comparison of methods that characterize pulses in a time series. *Statistics in Medicine* **14**, 311–325.

Merriam, G. R. and Wachter, K. W. (1982). Algorithms for the study of episodic hormone secretion. *American Journal of Physiology* **243**, 310–318.

Neal, R. M. (2000). Markov chain sampling methods for Dirichlet process mixture models. *Journal of Computational and Graphical Statistics* **9**, 249–265.

Oerter, K. E., Guardabasso, V., and Rodbard, D. (1986). Detection and characterization of peaks and estimation of instantaneous secretory rate for episodic pulsatile

hormone secretion. *Computers and Biomedical Research* **19**, 170–191.

O'Sullivan, F. O. and O'Sullivan, J. (1988). Deconvolution of episodic hormone data: an analysis of the role of season on the onset of puberty in cows. *Biometrics* **44**, 339–353.

Robert, C. P. (2001). *The Bayesian Choice*. 2nd edition. New York: Springer.

Rodbard, D., Rayford, P. L., and Ross, G. T. (1970). Statistical quality control. In McArthur, J. W. and Colton, T., editors, *Statistics in Endocrinology*, pages 411–429. Cambridge, MA: The MIT Press.

Stephens, M. (2000). Bayesian analysis of mixture models with an unknown number of components—an alternative to reversible jump methods. *Annals of Statistics* **28**, 40–74.

Van Cauter, E. L., et al. (1981). Quantitative analysis of spontaneous variation in plasma prolactin in normal man. *American Journal of Physiology* **241**, 355–363.

Veldhuis, J. D. and Johnson, M. L. (1986). Cluster analysis: a simple, versatile and robust algorithm for endocrine pulse detection. *American Journal of Physiology* **250**, 486–493.

Veldhuis, J. D. and Johnson, M. L. (1992). Deconvolution analysis of hormone data. In Brand, L. and Johnson, M. L., editors, *Methods in Enzymology*, pages 539–575. San Diego: Academic Press.

Veldhuis, J. D., et al. (1989). Amplitude modulation of a burstlike mode of cortisol secretion subserves the circadian glucocortocid rhythm in man. *American Journal of Physiology* **257**, 6–14.

Wahba, G. (1990). *Spline Models for Observational Data*. Philadelphia, PA.: Society for Industrial and Applied Mathematics.

Yang, Y., Liu, A., and Wang, Y. (In Press). Detecting pulsatile hormone secretions

using nonlinear mixed effects partial spline models. *Biometrics* .

Young, E. A., Carlson, N. E., and Brown, M. B. (2001). Twenty-four-hour ACTH and Cortisol pulsatility in depressed women. *Neuropsychopharmacology* **25**, 267–276.

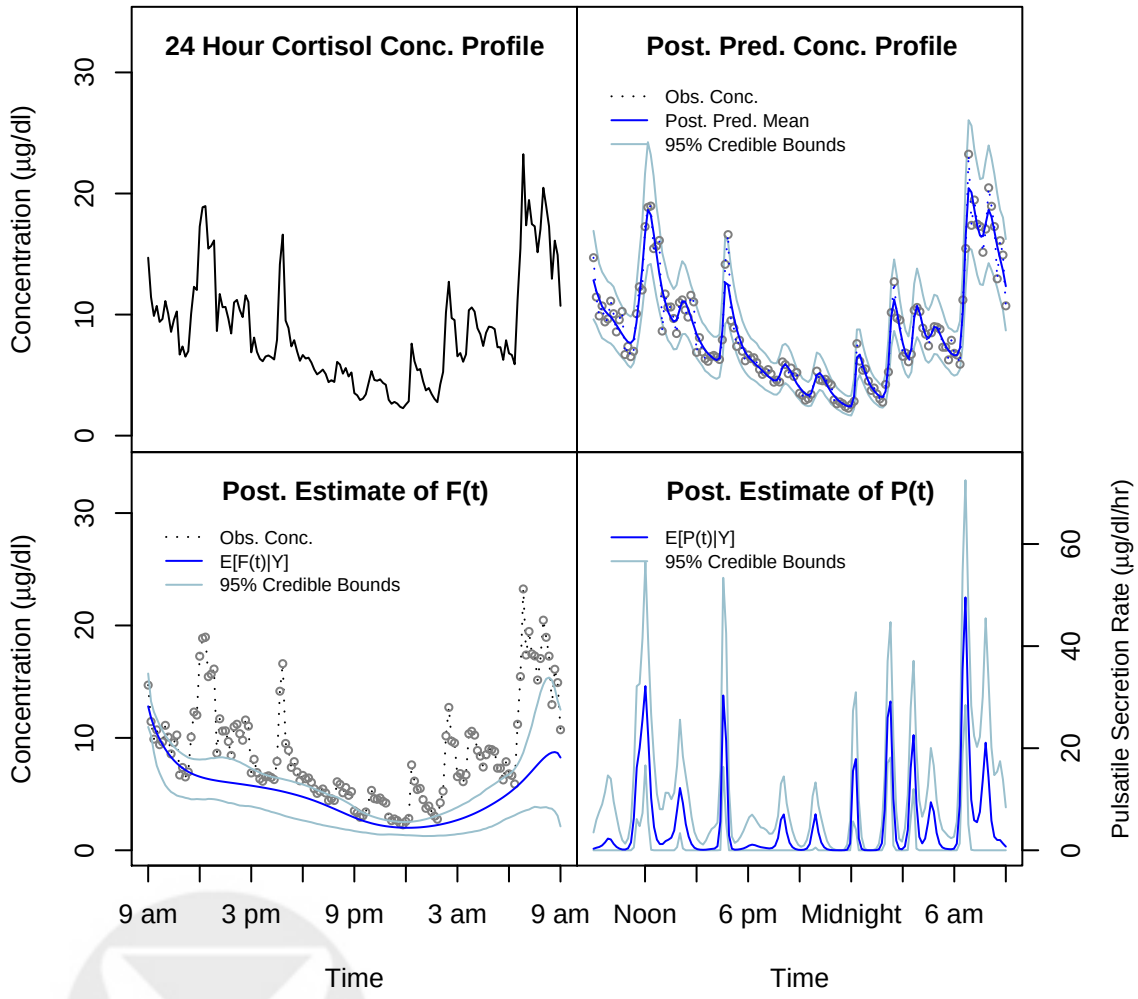

Figure 1: (UL) An example of cortisol concentrations from a female subject suffering from depression over a twenty-four hour time period. Note the pulsatile nature of the concentration. Plasma concentration levels of cortisol were obtained at ten minute intervals. (UR) Model fit to the data. (LL) Posterior mean of the nuisance function: $E(F(t) \mid Y)$. (LR) The posterior estimate of $P(t) \mid Y$.

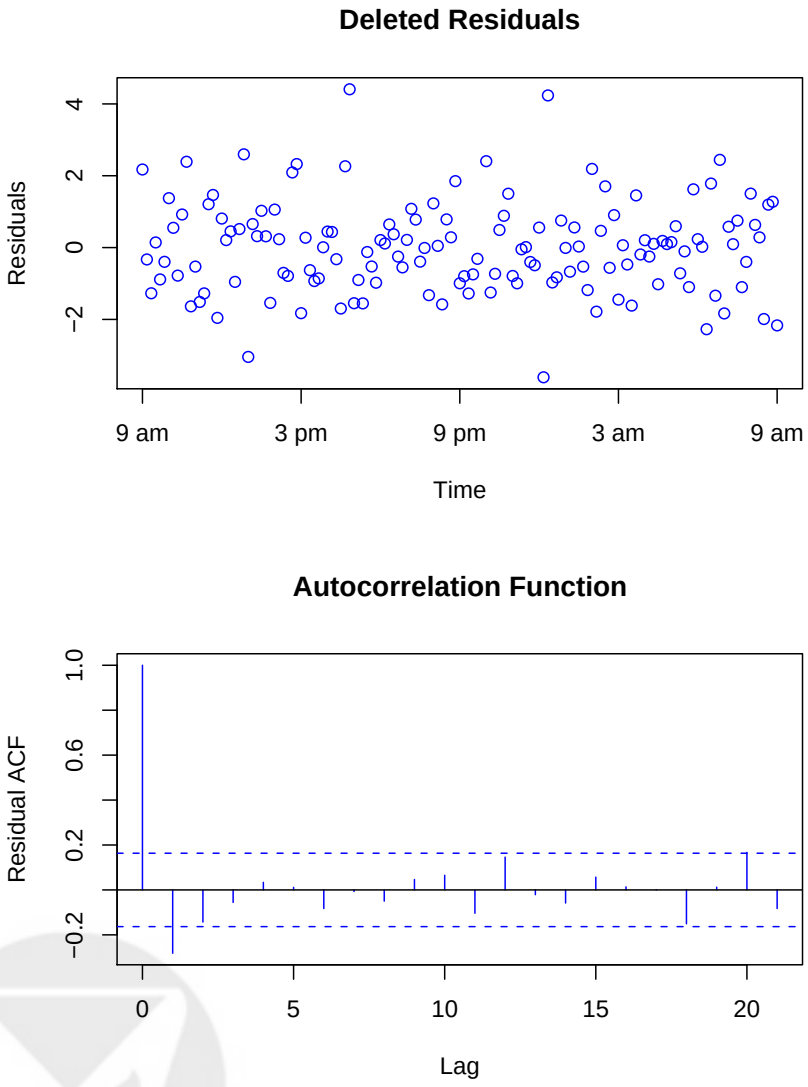

Figure 2: Bayesian deleted residuals and the autocorrelation function of the deleted residuals. No residual structure can be seen in the deleted residuals and no there is no autocorrelation in the residuals.

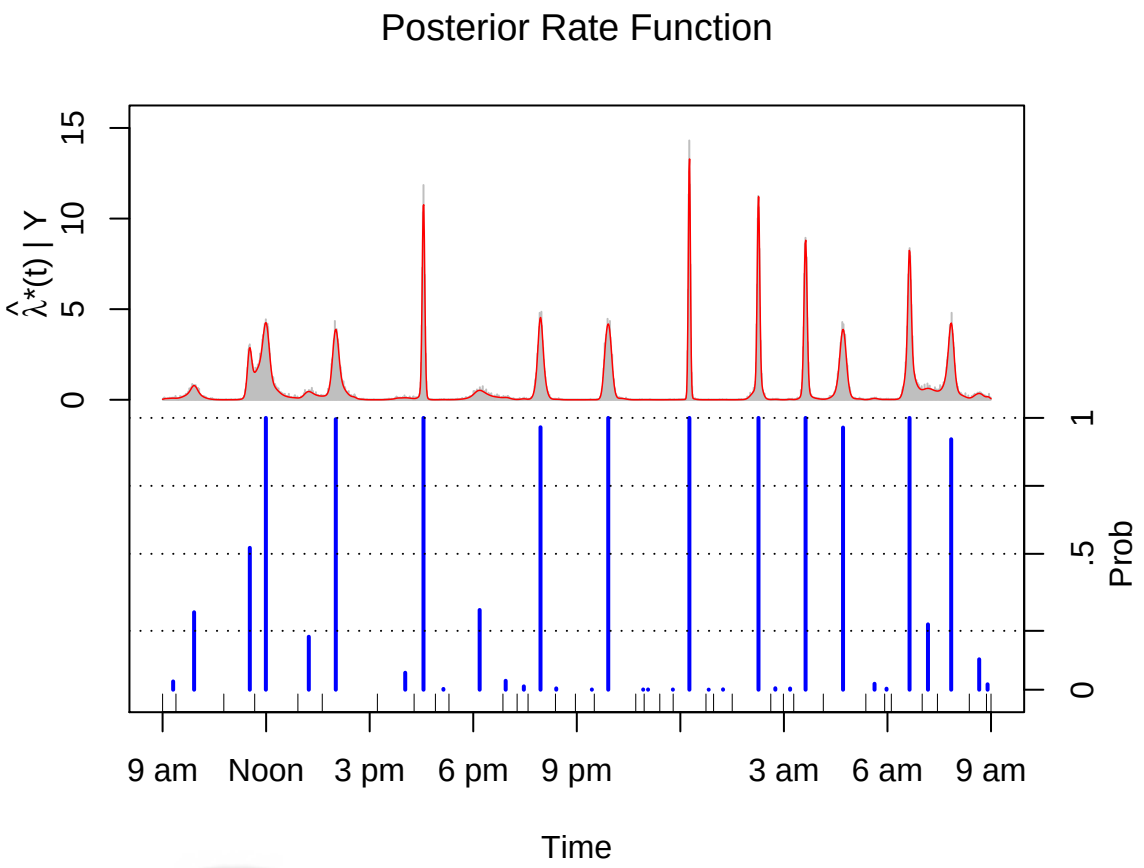

Figure 3: The top portion of this figure shows the estimated marginal posterior rate function, $\hat{\lambda}^*(t) \mid Y$, estimated from the MDP model. The blue lines in the bottom portion show locations of all local maxima and the probabilities (12). Some maxima are so small, they cannot be seen. The rug at the bottom shows the intervals endpoints (the local minima) on which the probabilities were estimated.

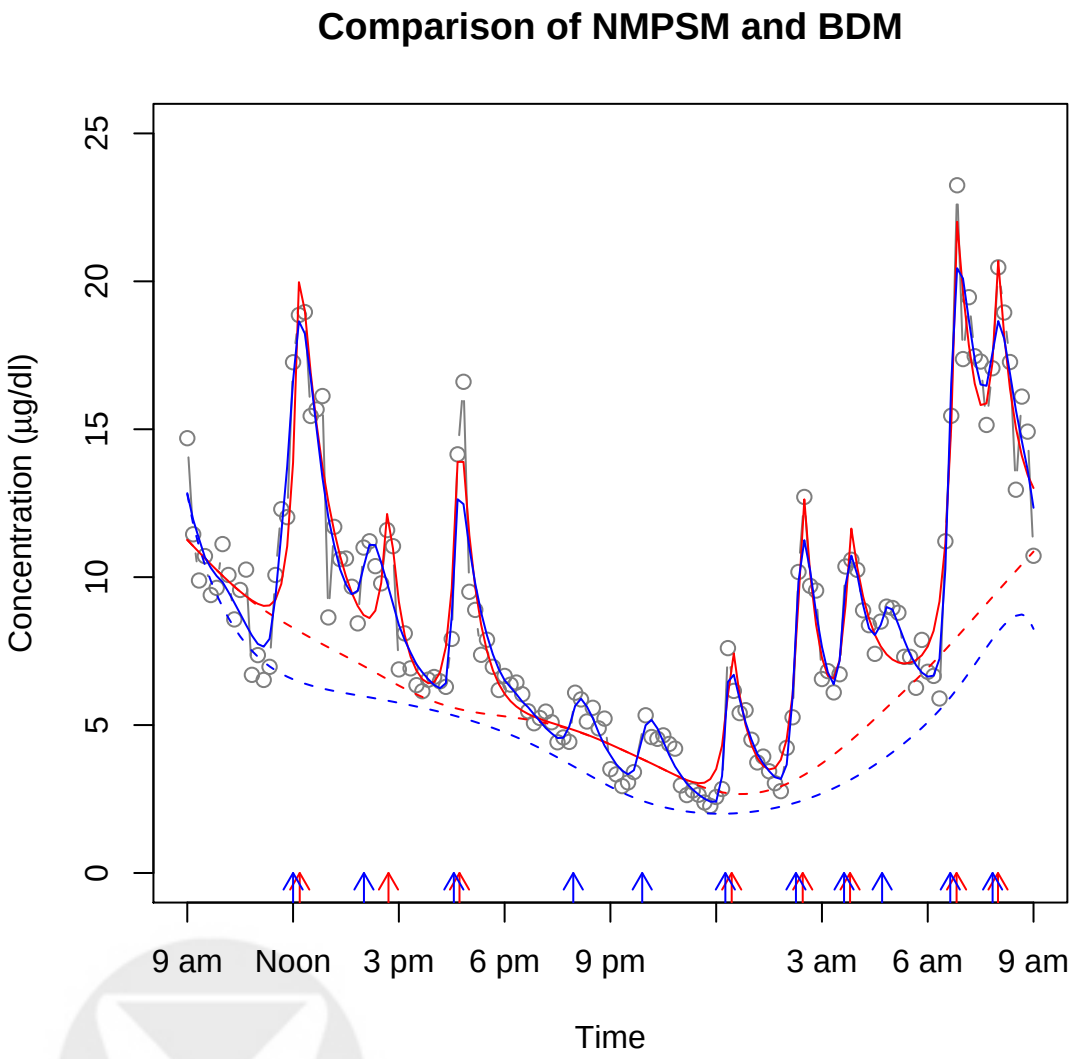

Figure 4: Comparison of the Bayesian deconvolution model and the NMPSM. The blue line is from the BDM, the red from NMPSM. The solid lines are the estimated concentration. The dashed lines are the estimated nuisance function. The arrows at the bottom show point estimates of event locations.